J|A|C|S ARTICLES

Published on Web 06/18/2010

Tuning the Supramolecular Chirality of One- and Two-Dimensional Aggregates with the Number of Stereogenic Centers in the Component Porphyrins

Patrizia Iavicoli,[†] Hong Xu,[‡] Lise N. Feldborg,[†] Mathieu Linares,[⊥,§,||] Markos Paradinas,[†] Sven Stafström,[||] Carmen Ocal,[†] Belen Nieto-Ortega,[#] Juan Casado,[#] Juan T. López Navarrete,[#] Roberto Lazzaroni,*[,§] Steven De Feyter,*[,‡] and David B. Amabilino*[,†]

Institut de Ciència de Materials de Barcelona (CSIC), Campus Universitari de Bellaterra, 08193 Cerdanyola del Vallès, Catalonia, Spain, Katholieke Universiteit Leuven, Laboratory of Photochemistry and Spectroscopy, and INPAC-Institute for Nanoscale Physics and Chemistry, Celestijnenlaan 200-F, 3001 Heverlee, Belgium, Service de Chimie des Matériaux Nouveaux, Université de Mons, 20, Place du Parc, B-7000 Mons, Belgium, Department of Physics, Chemistry and Biology, Linköping University, SE-581 83 Linköping, Sweden, and Departamento de Química Física, Facultad de Ciencias, Universidad de Málaga, Málaga 29071, Spain

Received February 22, 2010; E-mail: amabilino@icmab.es; steven.defeyter@chem.kuleuven.be; roberto.lazzaroni@umons.ac.be

Abstract: A synthetic strategy was developed for the preparation of porphyrins containing between one and four stereogenic centers, such that their molecular weights vary only as a result of methyl groups which give the chiral forms. The low-dimensional nanoscale aggregates of these compounds reveal the profound effects of this varying molecular chirality on their supramolecular structure and optical activity. The number of stereogenic centers influences significantly the self-assembly and chiral structure of the aggregates of porphyrin molecules described here. A scanning tunneling microscopy study of monolayers on graphite shows that the degree of structural chirality with respect to the surface increases almost linearly with the number of stereogenic centers, and only one handedness is formed in the monolayers, whereas the achiral compound forms a mixture of mirror-image domains at the surface. In solution, four hydrogen bonds induce the formation of an H-aggregate, and circular dichroism measurements and theoretical studies indicate that the compounds self-assemble into helical structures. Both the chirality and stability of the aggregates depend critically on the number of stereocenters. The chiral porphyrin derivatives gelate methylcyclohexane at concentrations dependent on the number and position of chiral groups at the periphery of the aromatic core, reflecting the different aggregation forces of the molecules in solution. Increasing the number of stereogenic centers requires more material to immobilize the solvent, in all likelihood because of the greater solubility of the porphyrins. The vibrational circular dichroism spectra of the gels show that all compounds have a chiral environment around the amide bonds, confirming the helical model proposed by calculations. The morphologies of the xerogels (studied by scanning electron microscopy and scanning force microscopy) are similar, although more fibrous features are present in the molecules with fewer stereogenic centers. Importantly, the presence of only one stereogenic center, bearing a methyl group as the desymmetrizing ligand, in a molecule of considerable molecular weight is enough to induce single-handed chirality in both the one- and two-dimensional supramolecular self-assembled structures.

Introduction

Chiral structures are interesting from a number of viewpoints,[1] and for this reason, the induction of chirality and its comprehension are worthy pursuits. While it has been established that the position of stereogenic centers clearly influences the sign and magnitude of optical activity in molecules united by covalent or noncovalent bonds,[2] the effect that the number of stereogenic centers in molecules has on the amplification of chirality in the aggregates that they form is (as far as we are aware) a largely unknown and unexplored area,[3] except from a very nice recent study[4] carried out in parallel to the work reported here, which explores this somewhat barren quarter.

[†] ICMAB-CSIC.
[‡] Katholieke Universiteit Leuven.
[§] Université de Mons.
[||] Linköping University.
[⊥] Present address: Department of Theoretical Chemistry, Royal Institute of Technology, Roslagstullsbacken 15, S-106 91, Stockholm, Sweden.
[#] Universidad de Málaga.

(1) (a) Crego-Calama, M., Reinhoudt, D. N., Eds. Supramolecular Chirality. In *Top. Curr. Chem.* **2006**, 26. (b) Soai, K., Ed. Amplification of Chirality. In *Top. Curr. Chem.* **2008**, 284. (c) Amabilino, D. B., Ed. *Chirality at the Nanoscale*; Wiley-VCH: Weinheim, 2009. (d) Raval, R. *Chem. Soc. Rev.* **2009**, *38*, 707–721. (e) Crassous, J. *Chem. Soc. Rev.* **2009**, *38*, 830–845.

 10.1021/ja101533j

The question of the influence of the number of stereogenic centers on chiral structure and optical activity is important because, while sergeants and soldiers[5] and majority rules[6] effects can drive chirality induction in supramolecular systems, the cases are relatively scarce, and it seems more habitual to find a linear dependence of optical activity on chiral content in achiral materials. The potential implications of understanding chiral induction are important because the relative disposition of molecules in condensates has profound effects on their properties, and the twist between chromophores is one key feature. In this regard, functional self-assembled molecular materials with well-defined shapes and dimensions are of great current interest,[7] especially for applications in electronics, photonics, light-energy conversion, and catalysis. In biological systems, tetrapyrrolic pigments are often self-organized into nanoscale superstructures that perform many of the essential light-harvesting and energy- and electron-transfer functions. An example is the light-harvesting rods of the chlorosomes of green-sulfur bacteria, which are composed entirely of aggregated bacteriochlorophyll.[8] Some synthetic porphyrins are known to form aggregates with interesting optical and electronic properties,[9] and these aggregates sometimes occur in the form of useful nanostructures including fibers, nanorods, or thin stripes on surfaces.[10] Therefore, because of their desirable functional properties, porphyrins and other tetrapyrroles are attractive building blocks for functional nanostructures,[11] as well as interesting chromophores for studies related to induction of chirality,[12] and are the core structures we have used in the studies reported here.

Bearing these considerations in mind, we designed and synthesized porphyrin derivatives **1**−**6** which contain amide groups as a simple hydrogen-bonding functional unit (Figure 1) and alkyl chains to provide solubility for the systems in solution as well as adhesion to each other and surfaces through van der Waals interactions. The compounds differ from each other in the number and position of the stereogenic centers they contain, and our aim was to investigate the role of these chiral centers in the formation of supramolecular 1-D and 2-D aggregate nanostructures. This study was done in solution using circular dichroism (CD) spectroscopy and at an interface by scanning tunneling microscopy (STM). The interpretation of the results was assisted by molecular mechanics (MM) and molecular dynamics (MD) simulations of the supramolecular assembly.[13] In addition, the ability of each one of these compounds to gelate organic solvents was investigated, and the characteristics of the gels and xerogels were explored by vibrational circular dichroism (VCD), scanning electron microscopy (SEM) and scanning force microscopy (SFM), respectively.

Result and Discussion

Synthesis and Characterization. The porphyrin derivatives **1**−**6** were prepared by the synthetic route described in Scheme

(2) See, for example: (a) Gray, G. W.; McDonnell, D. G. *Mol. Cryst., Liq. Cryst.* **1977**, *34*, 211–217. (b) Marcellis, A. T. M.; Koudijs, A.; Sudholter, E. J. R. *Liq. Cryst.* **1995**, *18*, 843–850. (c) Amabilino, D. B.; Ramos, E.; Serrano, J.-L.; Sierra, T.; Veciana, J. *J. Am. Chem. Soc.* **1998**, *120*, 9126–9134. (d) Yablon, D. G.; Wintgens, D.; Flynn, G. W. *J. Phys. Chem. B* **2002**, *106*, 5470–5475. (e) Umadevi, S.; Jakli, A.; Sadashiva, B. K. *Soft Matter* **2006**, *2*, 875–885. (f) Henze, O.; Feast, W. J.; Gardebien, F.; Jonkheijm, P.; Lazzaroni, R.; Leclere, P. K.; Meijer, E. W.; Schenning, A. P. H. J. *J. Am. Chem. Soc.* **2006**, *128*, 5923–5929. (g) Yang, Y. G.; Nakazawa, M. S.; Suzuki, M.; Shirai, H.; Hanabusa, K. *J. Mater. Chem.* **2007**, *17*, 2936–2943. (h) Zhi, J. G.; Zhu, Z. G.; Liu, A. H.; Cui, J. X.; Wan, X. H.; Zhou, Q. F. *Macromolecules* **2008**, *41*, 1594–1597.

(3) When considering aggregates, and while it is clear that the systems are either chiral or achiral globally, the optical activity and degree of structural chirality can vary, as in a liquid crystal, for example, where increasing content of a chiral dopant in an achiral liquid crystal gives structural twist and optical activity which depend on the concentration of the dopant (see, for example; Wilson, M. R.; Earl, D. J. *J. Mater. Chem.* **2001**, *11*, 2672–2677. On the other hand, work has been done to determine the degree of chirality of molecular systems; see: Mislow, K.; Buda, A. B.; Heyde, T. E. *Angew. Chem., Int. Ed. Engl.* **1992**, *31*, 989–1007. Alvarez, S.; Alemany, P.; Avnir, D. *Chem. Soc. Rev.* **2005**, *34*, 313–326.

(4) Smulders, M. M. J.; Stals, P. J. M.; Mes, T.; Paffen, T. F. E.; Schenning, A. P. H. J.; Palmans, A. R. A.; Meijer, E. W. *J. Am. Chem. Soc.* **2010**, *132*, 620–626.

(5) (a) Green, M. M.; Reidy, M. P. *J. Am. Chem. Soc.* **1989**, *111*, 6452–6454. (b) Gu, H.; Nakamura, Y.; Sato, T.; Teramoto, A.; Green, M. M.; Jha, S. K.; Andreola, C.; Reidy, M. P. *Macromolecules* **1998**, *31*, 6362–6368. (c) de Jong, J. J. D.; Tiemersma-Wegman, T. D.; van Esch, J. H.; Feringa, B. L. *J. Am. Chem. Soc.* **2005**, *127*, 13804–13805. (d) Wilson, A. J.; van Gestel, J.; Sijbesma, R. P.; Meijer, E. W. *Chem. Commun.* **2006**, 4404–4406. (e) Nam, S. R.; Lee, H. Y.; Hong, J.-I. *Chem.—Eur. J.* **2008**, *14*, 6040–6043. (f) Smulders, M. M. J.; Schenning, A. P. H. J.; Meijer, E. W. *J. Am. Chem. Soc.* **2008**, *130*, 606–611.

(6) (a) Green, M. M.; Peterson, N. C.; Sato, T.; Teramoto, A.; Cook, R.; Lifson, S. *Science* **1995**, *268*, 1860–1866. (b) Green, M. M.; Garetz, B. A.; Munoz, B.; Chang, H.; Hoke, S.; Cooks, R. G. *J. Am. Chem. Soc.* **1995**, *117*, 4181–4182. (c) Langeveld-Voss, B. M. W.; Waterval, R. J. M.; Janssen, R. A. J.; Meijer, E. W. *Macromolecules* **1999**, *32*, 227–230. (d) van Gestel, J.; Palmans, A. R. A.; Titulaer, B.; Vekemans, J. A. J. M.; Meijer, E. W. *J. Am. Chem. Soc.* **2005**, *127*, 5490–5494.

(7) (a) Elemans, J. A. A. W.; Van Hameren, R.; Nolte, R. J. M.; Rowan, A. E. *Adv. Mater.* **2006**, *18*, 1251–1266. (b) Gomar-Nadal, E.; Puigmartí-Luis, J.; Amabilino, D. B. *Chem. Soc. Rev.* **2008**, *37*, 490–504. (c) Yagai, S.; Kitamura, A. *Chem. Soc. Rev.* **2008**, *37*, 1520–1529. (d) Meng, Q.; Sun, X.-H.; Lu, Z.; Xia, P.-F.; Shi, Z.; Chen, D.; Wong, M. S.; Wakim, S.; Lu, J.; Baribeau, J.-M.; Tao, Y. *Chem.—Eur. J.* **2009**, *15*, 3474–3487. (e) Alesi, S.; Brancolini, G.; Viola, I.; Capobianco, M. L.; Venturini, A.; Camaioni, N.; Gigli, G.; Melucci, M.; Barbarella, G. *Chem.—Eur. J.* **2009**, *15*, 1876–1885. (f) An, B. K.; Gihm, S. H.; Chung, J. W.; Park, C. R.; Kwon, S. K.; Park, S. Y. *J. Am. Chem. Soc.* **2009**, *131*, 3950–3957.

(8) (a) Staehelin, L. A.; Golecki, J. R.; Fuller, R. C.; Drews, G. *Biophys. J.* **1978**, *85*, 3173–3186. (b) van Rossum, V.-J.; Steensgaard, D. B.; Mulder, F. M.; Boender, G. J.; Schaffner, K.; Holzwarth, A. R.; de Groot, H. J. M. *Biochemistry* **2001**, *40*, 1587–1595. (c) Blankenship, R. E.; Olson, J. M.; Miller, M. In *Antenna Complexes from Green Photosynthetic Bacteria*; Blankenship, R. E., Madigan, M. T., Bauer, C. E., Eds.; Kluwer Academic Publishers: Dordrecht, The Netherlands, 1995; pp 339−435. (d) Olson, J. M. *Photochem. Photobiol.* **1998**, *67*, 61–75. (e) Egawa, A.; Fujiwara, T.; Mizoguchi, T.; Kakitani, Y.; Koyama, Y.; Akutsu, H. *Proc. Natl. Acad. Sci. U.S.A.* **2007**, *104*, 795–799.

(9) (a) Marks, T. J. *Science* **1985**, *227*, 881–889. (b) Chen, Y. C.; Lee, M. W.; Li, L. L.; Lin, K. J. *J. Macromol. Sci. B Phys.* **2008**, *47* (5), 955–966. (c) Aziz, M. S. *Solid-State Electron.* **2008**, *52*, 1145–1148.

(10) (a) Fuhrhop, J.-H.; Binding, U.; Siggel, U. *J. Am. Chem. Soc.* **1993**, *115*, 11036–11037. (b) Schwab, A. D.; Smith, D. E.; Rich, C. S.; Young, E. R.; Smith, W. F.; de Paula, J. C. *J. Phys. Chem. B* **2003**, *107*, 11339–11345. (c) Rotomskis, R.; Augulis, R.; Snitka, V.; Valiokas, R.; Liedberg, B. *J. Phys. Chem. B* **2004**, *108*, 2833–2838. (d) Koepf, M.; Wytko, J. A.; Bucher, J. P.; Weiss, J. *J. Am. Chem. Soc.* **2008**, *130*, 9994–10001.

(11) (a) Nakamura, Y.; Aratani, N.; Osuka, A. *Chem. Soc. Rev.* **2007**, *36*, 831–845. (b) Yamamoto, S.; Watarai, H. *J. Phys. Chem. C* **2008**, *112*, 12417–12424. (c) In't Veld, M.; Iavicoli, P.; Haq, S.; Amabilino, D. B.; Raval, R. *Chem. Commun.* **2008**, 1536–1538. (d) Faiz, J. A.; Heitz, V.; Sauvage, J. P. *Chem. Soc. Rev.* **2009**, *38*, 422–442.

(12) (a) Rubires, R.; Crusats, J.; El-Hachemi, Z.; Jaramillo, T.; López, M.; Valls, E.; Farrera, J.-A.; Ribó, J. M. *New J. Chem.* **1999**, 189–198. (b) Rubires, R.; Farrera, J.-A.; Ribó, J. M. *Chem.—Eur. J.* **2001**, *7*, 436–446. (c) Escudero, C.; Crusats, J.; Diez-Perez, I.; El-Hachemi, Z.; Ribó, J. M. *Angew. Chem., Int. Ed.* **2006**, *45*, 8032–8035. (d) Randazzo, R.; Mammana, A.; D'Urso, A.; Lauceri, R.; Purrello, R. *Angew. Chem., Int. Ed.* **2008**, *47*, 9879–9882. (e) Rosaria, L.; D'Urso, A.; Mammana, A.; Purrello, R. *Chirality* **2008**, *20*, 411–419. (f) El-Hachemi, Z.; Escudero, C.; Arteaga, O.; Canillas, A.; Crusats, J.; Manzini, G.; Purrello, R.; Sorrenti, A.; D'urso, A.; Ribo, J. M. *Chirality* **2009**, *21*, 408–412.

(13) MM and MD calculations were performed with the tinker package (http://dasher.wustl.edu/tinker/) and the MM3 force field: Allinger, N. L.; Yuh, Y. H.; Lii, J. H. *J. Am. Chem. Soc.* **1989**, *111*, 8551–8566.

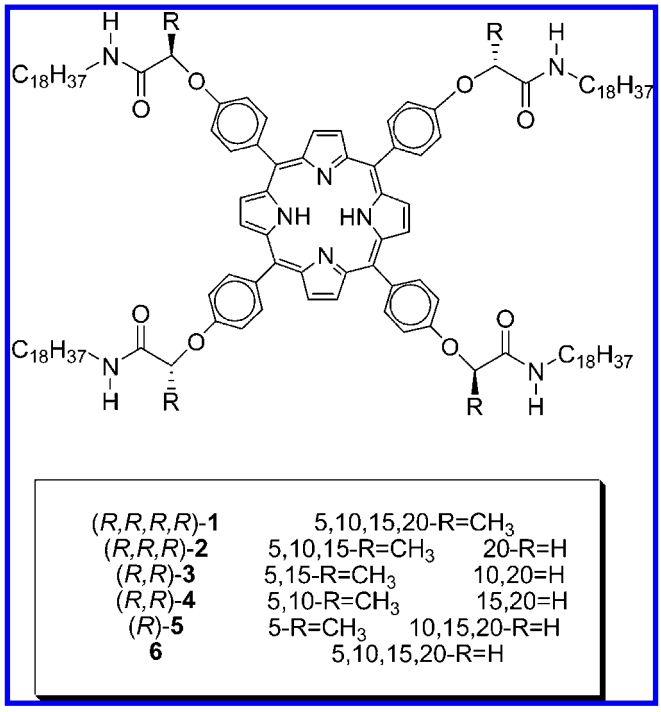

Figure 1. Chemical structures of the compounds prepared and studied in this work. Both the *R* and *S* enantiomers of the chiral compounds were synthesized, but only the *R* enantiomers are discussed here.

1. All of the discussion here refers to the *R* enantiomers, but we also prepared the *S* enantiomers, which give equal and opposite chirostructural and chiroptical effects.

This strategy was carefully chosen so as to be able to separate the different compounds with one, two, and three stereogenic centers and the constitutional isomers of the compounds with two stereogenic compounds from each other after the one-pot reaction used to make all the intermediate porphyrins **9**−**13**. The long alkyl chain in one of the aldehydes in this condensation reaction with pyrrole makes the products sufficiently different so as to allow their isolation by silica gel column chromatography. Thus, (*R*)-methyl 2-(4-formylphenoxy)propionate ((*R*)-**7**)[14] and 2-(4-formylphenoxy)-*N*-octadecylacetamide (**8**), prepared by the reaction of 4-hydroxybenzaldehyde and *N*-octadecyl-2-chloroacetamide[15] (see the Experimental Section in the Supporting Information) were condensed with pyrrole in refluxing propionic acid in air to give the corresponding chiral porphyrin derivatives **9**−**13** and the achiral porphyrin **6**. These compounds were separated from one another by extensive column chromatography and were characterized by different spectroscopic techniques in order to distinguish them from one another (see the Experimental Section in the Supporting Information).

In particular, the IR spectra of solids **10**−**13** showed two signals from the carbonyl moiety of the ester group at 1756 and 1739 cm^{-1} and one peak from the equivalent bond in the amide group. The relative intensity of the peaks corresponding to the two different groups changes with their number in each molecule, and the peak from the carbonyl moiety in the amide group changes position with the number of amide groups in

Scheme 1. Synthesis of the Porphyrin Derivatives **1**−**6**

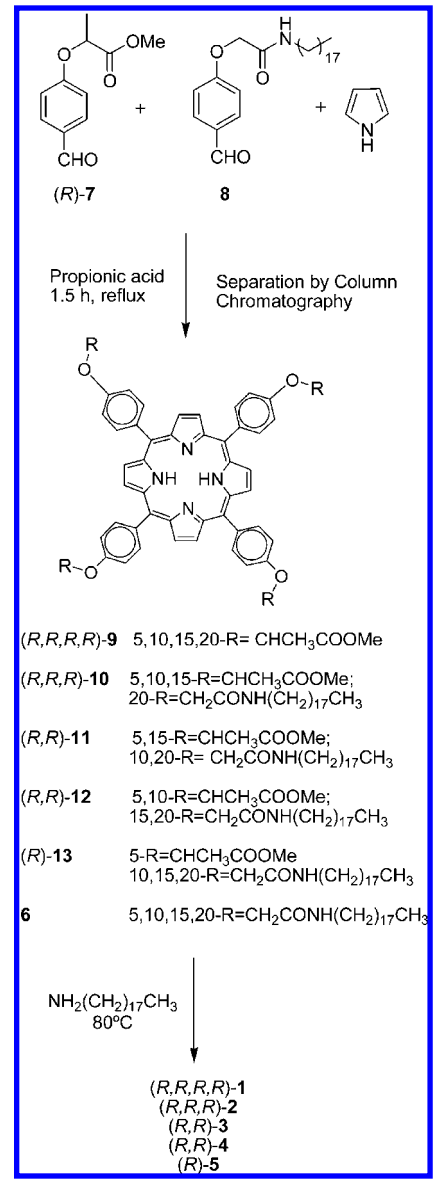

the molecule and so with the amount of specifically aggregated molecules in the solid state. With an increasing number of amide groups there is a general shift to lower frequency of the peak of the amide group in the solids (1679 cm^{-1} for (*R,R,R*)-**10**, 1672 for (*R,R*)-**11**, 1666 for (*R,R*)-**12**, 1672 for (*R*)-**13**, and 1655 cm^{-1} for **6**).

It was challenging to distinguish between the constitutional isomers (*R,R*)-**11** and (*R,R*)-**12**. The first eluted sample from the column was expected to be the less polar 5,15 porphyrin derivative (*R,R*)-**11**, but the ^{1}H NMR spectra measured at room temperature were virtually identical to those of the next eluted porphyrin, the two having identical mass spectra. While the ^{1}H NMR spectra measured at room temperature show a double doublet resonance for the hydrogen atoms of the pyrrole groups for both fractions, when the spectrum was run at 60 °C (when the rate of interconversion of the hydrogen atoms attached to the pyrrole nitrogen atoms is apparently sufficiently faster than the NMR time scale so that a well-resolved averaged spectrum results) compound (*R,R*)-**11** gave a clear double doublet and compound (*R,R*)-**12** gave a double doublet with two singlets almost overlapping the inner peaks of the doublets

(14) Minguet, M.; Amabilino, D. B.; Vidal-Gancedo, J.; Wurst, K.; Veciana, J. *J. Mater. Chem.* **2002**, *12*, 570–578.
(15) Puigmartí-Luis, J.; Minoia, A.; Pérez del Pino, A.; Ujaque, G.; Rovira, C.; Lledos, A.; Lazzaroni, R.; Amabilino, D. B. *Chem.—Eur. J.* **2006**, *12*, 9161–9175.

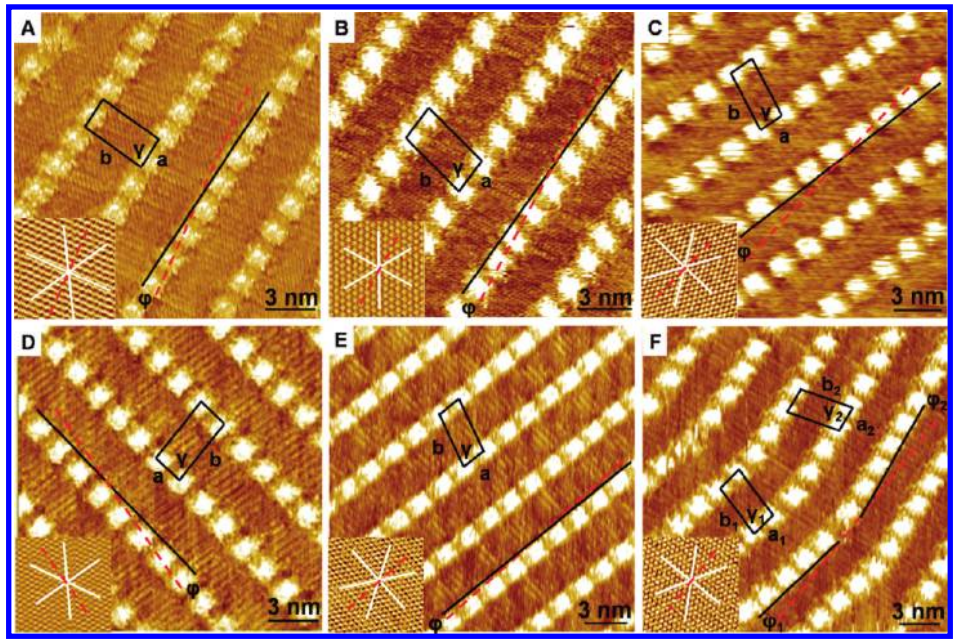

Figure 2. STM images of porphyrin derivatives **2**−**6** physisorbed at the HOPG−1-heptanol interface (I_{set} = 0.6 nA; V_{set} = −0.2 V): (A) (*R,R,R*)-**2**, (B) (*R,R*)-**3**, (C) (*R,R*)-**4**, (D) (*S,S*)-**4**, (E) (*R*)-**5**, (F) **6**. The insets show STM images of HOPG (not to scale) corresponding to sites underneath the monolayer (I_{set} =0.6 nA; V_{set} = −0.001 V). The solid white lines in the insets indicate the direction of the main symmetry axis of HOPG. The dashed red lines in all insets and main images are the selected HOPG reference axes <−1 1 0 0>. Unit cells are indicated in black. The solid black line is the propagation axis of the porphyrin rows. φ is the angle between the reference axis and the propagation axis. Each inset relates to the area underneath the monolayer.

(see the Supporting Information). Even at room temperature, the exchange is sufficiently slow so as to broaden the spectrum so that definitive assignment cannot be achieved.

The ester groups adjacent to the stereogenic centers in the porphyrin derivatives **9**−**13** were subsequently amidated by mixing the compounds with octadecyl amine and heating to 80 °C using the latter as solvent. This procedure afforded the chiral amides **1**−**5** in quite respectable yields (around 85%) after thorough purification by column chromatography. The absorption spectra were the typical ones of free base porphyrins, and the ^{1}H NMR spectra showed all the resonances characteristic of the desired compounds. Mass spectra and elemental analysis were also in accord with the target compounds.

It is perhaps worthy of attention that the difference in molecular mass of the compounds with between one and four stereogenic centers is only 55 Da (the molecular masses range between 1917 and 1974 Da, respectively), so there is a less than 3% mass difference.[16] This value is interesting to be borne in mind given the quite dramatic effects that are seen in their assembly characteristics.

Investigation on the Structural Chirality of the Monolayers Formed at the Solid−Liquid Interface. The assembly of porphyrins **1**−**6** was studied at the highly oriented pyrolytic graphite (HOPG)−1-heptanol interface by dissolving the compounds in the solvent, applying a drop of the solution to a graphite slab, and performing the STM imaging of the interface with the tip of the microscope inserted into the solution.[17] Inspection of the resulting STM images permits the chiral nature of the domains to be recognized by the oblique shape of the unit cell.[18] The monolayers that are formed are not chiral globally because of the presence of enantiomeric domains.

For the present system, a better approach to probe molecule-based two-dimensional chirality is by evaluating the monolayer chirality by comparing its orientation versus graphite; i.e., the angle (φ) between the normal of a main symmetry axis of HOPG, i.e., the HOPG reference axis <−1 1 0 0> and unit cell vector **a**. In a previous STM study, we showed that the porphyrin rows of compound **1** self-assembled at the HOPG−1-heptanol interface do not run parallel to the reference axis of the substrate but exhibit an angle of approximately +13 ± 2° with respect to that direction.[19] The same orientation is observed in all domains probed: The porphyrin rows are always rotated clockwise with respect to the reference axis for the *R* enantiomer. This result indicates clearly that the stereogenic centers influence strongly the molecule−surface interaction in the monolayers of **1**, an assertion backed up by modeling.[19] Therefore, the degree of chiral induction might not be optimum. For this reason, a key question remaining from that study was how the amount of chiral information at the molecular level is transferred and expressed structurally at the monolayer level. In order to try to answer to this question, we analyzed the self-assembly of compounds **2**−**6** (together with the (*S*) enantiomers) at the same interface to discover how the angle formed by the monolayer with respect to the substrate is affected by the number and location of stereogenic centers in the molecule (Figure 2). The solvent was always 1-heptanol, as the solvent plays a crucial

(16) To make the masses identical, additional carbon atoms would have to be added at some location in the compounds, perhaps most logically in the alkyl chains. However, this modification would give rise to odd−even effects in the assembly.

(17) Elemans, J. A. A. W.; De Cat, I.; Xu, H.; De Feyter, S. *Chem. Soc. Rev.* **2009**, *38*, 722–736.

(18) (a) Qiu, X.; Wang, C.; Zeng, Q.; Xu, B.; Yin, S.; Wang, H.; Xu, S.; Bai, C. *J. Am. Chem. Soc.* **2000**, *122*, 5550–5556. (b) Zhou, Y.; Wang, B.; Zhu, M.; Hou, J. G. *Chem. Phys. Lett.* **2005**, *403*, 140–145. (c) Otsuki, J.; Nagamine, E.; Kondo, T.; Iwasaki, K.; Asakawa, M.; Miyake, K. *J. Am. Chem. Soc.* **2005**, *127*, 10400–10405.

(19) Linares, M.; Iavicoli, P.; Psychogyiopoulou, K.; Beljonne, D.; De Feyter, S.; Amabilino, D. B.; Lazzaroni, R. *Langmuir* **2008**, *24*, 9566–9574.

Table 1. Unit Cell Parameters (a, b, γ), Angles of Direction of Unit Cell Vector **a** with Respect to the HOPG Reference Axis <−1 1 0 0 > (φ), and Numbers of Domains Investigated of **1**−**6** at the HOPG−1-Heptanol Interface (**n**)[a]

	n	*a* (nm)	*b* (nm)	γ (deg)	φ (deg)	φ_{MD} (deg)
(*R*,*R*,*R*,*R*)-**1**	29	1.9 ± 0.1	4.0 ± 0.1	80 ± 2	+13 ± 4	12.2 ± 0.4
(*R*,*R*,*R*)-**2**	13	2.0 ± 0.1	4.2 ± 0.3	80 ± 5	+10 ± 3	10.2 ± 0.2
(*R*,*R*)-**3**	21	1.9 ± 0.1	4.1 ± 0.1	80 ± 2	+7 ± 2	7.5 ± 0.2
(*R*,*R*)-**4**	8	1.9 ± 0.1	4.0 ± 0.1	81 ± 4	+9 ± 4	10.1 ± 0.3
(*R*)-**5**	19	1.9 ± 0.1	4.1 ± 0.1	79 ± 4	+7 ± 4	8.0 ± 0.3
6	6	2.0 ± 0.2	4.1 ± 0.2	79 ± 4	+6 ± 4	6.9 ± 0.4
	5	1.9 ± 0.1	4.3 ± 0.3	75 ± 3	−8 ± 2	
(*S*,*S*)-**4**	9	1.9 ± 0.1	4.1 ± 0.1	82 ± 3	−8 ± 2	

[a] As achiral molecule **6** forms two types of domains with $\varphi > 0$ and $\varphi < 0$, values for these domains are treated separately. φ_{MD} is the result of a molecular dynamics simulation.

role in the formation of this type of physisorbed self-assembled monolayers.[20]

The monolayers revealed some dynamics immediately after all of the porphyrin solutions were deposited on HOPG. Therefore, all images were captured at least 1 h after deposition. As shown in Figure 2, each compound self-assembles at the HOPG−1-heptanol interface forming nice patterns of ordered rows of molecules. The organization of molecules and the unit cell parameters are the same (within error) as those measured for **1** (Table 1). Importantly, the monolayers are essentially isostructural, with the porphyrin units adopting a coparallel orientation with respect to the surface and the alkyl chains extending away from the core and interdigitated with those coming from adjacent rows. This fact allows us to compare directly the influence of the number of stereogenic centers on the angle formed by the superstructure with respect to the surface.

The only discernible difference in the monolayers of compounds **1**−**6** is the angle that the lamellae form with respect to the graphite reference axis. Although all the layers present lamellae with positive angles for the *R* enantiomers, the average value decreases with the diminishing of the number of chiral centers in the molecules (Table 1).

The achiral molecule **6** has an average angle φ of about 0° over all domains, but for a given domain the angle of the rows with respect to the graphite reference axis is approximately 7°. Therefore, the achiral chain does not favor an achiral arrangement on the surface, but spontaneous resolution of conformers is observed.[21]

Though the positions of the chiral centers in compounds **3** and **4** are different, no obvious packing differences are observed. STM images of (*S*,*S*)-**4** (Figure 2) show that the molecular packing appears as mirror image of the enantiomer (*R*,*R*)-**4**.

All these data seem to indicate that the chiral centers have no major influence on the overall monolayer structure, except for the fact they select only one of the equivalent mirror-image patterns. A molecular modeling study was undertaken in order to put this hypothesis to test. The molecular rows of porphyrin **1** self-assembled at the HOPG−1-heptanol interface present an angle of +13 ± 2° (observed with STM) with respect to a reference axis of the substrate.[19] Calculations showed an angle

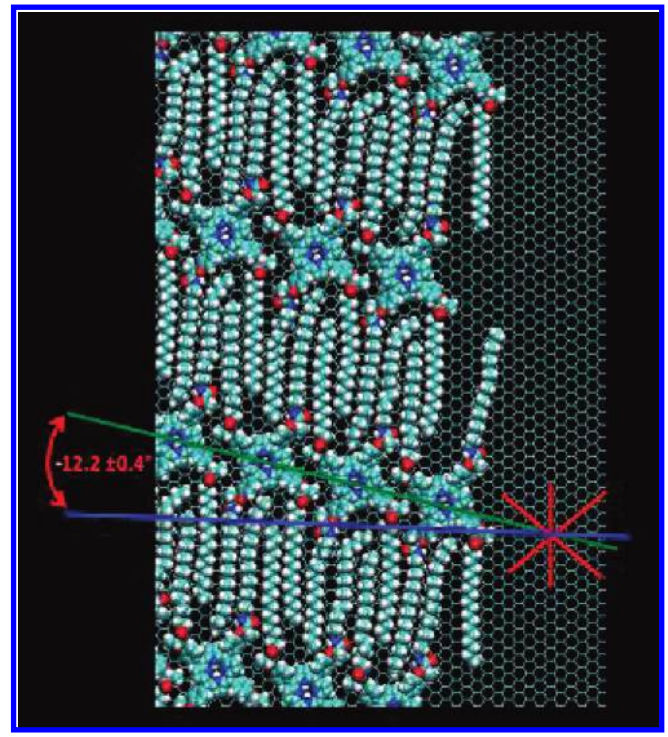

Figure 3. Snapshot from an MD simulation illustrating the deviation of rows of molecules (*R*,*R*,*R*,*R*)-**1** (green line) with respect to the reference axis of the graphite substrate (blue line). The reference axis runs perpendicular to one main axis of the graphite (red line).

of deviation of +12.2 ± 0.4°, in excellent agreement with experiment (see Figure 3).

This deviation originates from a specific adsorption of the porphyrin molecules on the surface, with the methyl group of the stereogenic centers pointing toward the surface and thus forcing a lateral shift of the porphyrin core of the adjacent molecule.[22] Starting from the self-assembly here obtained for porphyrin **1**, the methyl group on one chiral center was replaced by a hydrogen atom to study the deviation for the molecular rows of porphyrin **2**. We then performed MD simulations in the NVT canonical ensemble (constant number of particles, volume and temperature) at 300 K. The system was first equilibrated by running a 100 ps MD simulation, and the deviation of the porphyrin rows with respect to the graphite reference axis was then investigated in a 100 ps long MD run (with frames recorded every 0.1 ps). The same strategy was applied to study the deviation with respect to the reference axis for compounds **3**−**6** by replacing sequentially all the methyl groups. The calculated values are reported in Table 1, together with the experimental data.

A very good agreement exists between the calculated and the experimental values for the deviation of porphyrin rows with respect to the reference axis. This clearly confirms that the number of chiral centers on these porphyrin compounds increases the deviation with respect to the reference axis, which is a measurement of the chirality at the nanoscale. The origin

(20) Yang, Y.; Wang, C. *Curr. Opin. Colloid Interface Sci.* **2009**, *14*, 135–147.

(21) This situation is common for this type of monolayer; see: (a) Pérez-García, L.; Amabilino, D. B. *Chem. Soc. Rev.* **2002**, *31*, 342–356. (b) Pérez-García, L.; Amabilino, D. B. *Chem. Soc. Rev.* **2007**, *36*, 941–967.

(22) Computationally, the determination of the deviation of rows of porphyrins with respect to the reference axis is a delicate task because of commensurability issues between the layer and the substrate. One can use simulations under periodic boundary conditions (PBC) to determine the self-assembly cell parameters, but PBC must be removed to study the deviation with respect to a reference axis. See: Linares, M.; Minoia, A.; Brocorens, P.; Beljonne, D.; Lazzaroni, R. *Chem. Soc. Rev.* **2009**, *38*, 806–816.

of the increased angle appears to be the space required by the methyl group on the surface, which forces a displacement of one porphyrin core with respect to the adjacent ones. This effect is apparently averaged out over the monolayers, as in the molecules with a low number of stereogenic centers the lamellae still have regular packing on the surface.

Solution-State Studies of Porphyrins and Their Aggregates. The porphyrins reported here were also designed to be able to self-assemble into one-dimensional aggregates in solution through hydrogen bonds. Absorption spectroscopy is ideally suited for the study of the aggregates because the spectra of porphyrins are dominated by the electronic $\pi-\pi^*$ transitions associated with the aromatic chromophore.[23] The most intense band in the UV−visible range (the Soret band or B band) appears at around 420 nm with an extinction coefficient over 10^4 mol L^{-1} cm^{-1} for related compounds,[24] and it is associated with two quasidegenerate transitions oriented perpendicular to each other. This absorption band proved to be the most informative for the investigation of these compounds. UV−vis absorption measurements of all compounds in chloroform showed a Soret band at 421 nm, indicating that these molecules were behaving as isolated chromophores in the solution. The absorption spectra of the same compounds in methylcyclohexane showed a slightly blue-shifted Soret band at 419 nm (the shift is most likely caused by solvent polarity difference when compared with chloroform) and a shoulder at 400 nm (not present in the chloroform spectra) which is caused by exciton coupling between porphyrin units (see the Supporting Information). Exciton theory[25] suggests that a blue shift of the Soret band implies that the porphyrins are overlapped and parallel to each other[26] (the bathochromic and hypsochromic shifts correspond to the edge-to-edge (*J* aggregates) and face-to-face (*H* aggregates) aggregations, respectively). At room temperature, the shoulder at approximately 400 nm corresponding to the aggregated porphyrins is much more evident for compounds **5** and **6**, which assemble most strongly in solution while still displaying the Soret band at 419 nm from the solvated porphyrins that are isolated from one another (Figure 4). The remaining compounds show only the absorption bands corresponding to the nonaggregated porphyrins. The spectra in chloroform and methylcyclohexane for compounds **1**−**4** are virtually identical at room temperature, 5×10^{-6} M.

CD spectroscopy was used to obtain more information about the self-assembly of the molecules and especially the twisted orientation adopted between them.[27] In general, there is a direct correlation between the regions of absorption and the Cotton effects observed in CD. In the case of noncoupled chromophores, the shapes of the two spectra are similar, although the vibrational fine structure can be different. If two or more

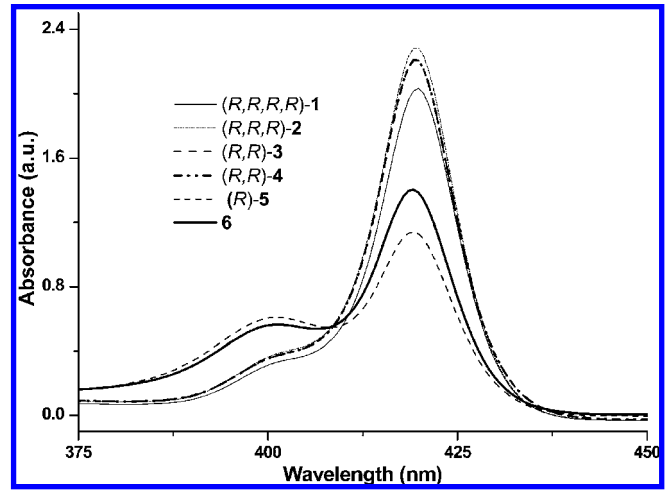

Figure 4. UV−vis absorption spectrum of compounds **1**−**6** (the spectra of **3** and **4** overlap perfectly) at room temperature in methylcyclohexane (5×10^{-6} M) showing the increase of the shoulder at 400 nm with decreasing number of stereogenic centers. The absorption band at 420 nm corresponds to nonaggregated porphyrins and the exciton band that appears as a shoulder at 400 nm corresponds to their H-aggregates.

strongly absorbing (identical) chromophores are oriented chirally with respect to each other, an exciton spectrum is observed and the wavelength at which the maximum in absorption occurs (λ_{max}) corresponds closely to zero in CD intensity. The latter case is rather frequent during the formation of helical aggregates which are a not infrequent basis of gel formation. During the self-assembly processes leading to gel formation, the CD spectrum undergoes dramatic modifications.[28] If two or more porphyrins are located nearby in space, the spectral region around 400 nm shows the coupling between the B transitions. The extent of any kind of interaction between electronic transitions is directly proportional to their intensity and inversely proportional to the energy difference.

Solutions of compounds **1**−**6** in methylcyclohexane were prepared (at a concentration of 1×10^{-5} M), and the CD spectra were measured at different temperatures between +25 and −10 °C (see the Supporting Information for all data). It is important to note that at least 20 min was necessary for the CD signal to stabilize, indicating a clear kinetic effect on the formation of the aggregates.

The enantiomers of compound **1** gave mirror image CD curves with a very weak Cotton effect at the position of the Soret band for all the temperatures studied, which accompanied by the lack of any change in the absorption spectra indicates that it does not associate under these conditions. At the other extreme, compound **6** could only be studied at 25 °C (below this temperature it precipitates) and shows a flat CD spectrum, as expected because of its achiral nature, and only shows noise in the region around the wavelength of the Soret band. Neither spontaneous symmetry breaking nor linear dichroic effects were ever observed.

While the solutions of compounds **2**−**5** were cooled, absorption spectra displayed a decrease in the intensity of the Soret band and a blue-shifted peak related to the aggregated form growth, along with distinctly bisignate CD signals with negative and positive Cotton effects measured at −10 °C (Table 2). This

(23) Ghosh, A. In *The Porphyrin Handbook*; Kadish, K. M., Smith, K. M., Guilard, R., Eds.; Academic Press: New York, 1978; Vol. III, pp 1−165.
(24) Iavicoli, P.; Simón-Sorbed, M.; Amabilino, D. B. *New J. Chem.* **2009**, *33*, 358–365.
(25) (a) McRae, G. M.; Kasha, M. *J. Chem. Phys.* **1958**, *28*, 721–722. (b) Kasha, M.; Rawls, H. R.; Ashraf El-Bayoumi, M. *Pure Appl. Chem.* **1965**, *11*, 371–392. (c) Kasha, M. In *Spectroscopy of the Excited State*; Bartolo, B. D., Ed.; Plenum: New York, 1976; pp 337−363.
(26) Hunter, C. A.; Sanders, J. K. M. *J. Am. Chem. Soc.* **1990**, *112*, 5525–5534.
(27) (a) Mammana, A.; D'Urso, A.; Lauceri, R.; Purrello, R. *J. Am. Chem. Soc.* **2007**, *129* (26), 8062–8063. (b) Wei, Y.; Zhanshuang, L.; Tianyu, W.; Minghua, L. *J. Colloid Interface Sci.* **2008**, *326*, 460–464. (c) Hoeben, F. J. M.; Wolffs, M.; Zhang, J.; De Feyter, S.; Leclère, P.; Schenning, A. P. H. J.; Meijer, E. W. *J. Am. Chem. Soc.* **2007**, *129*, 9819–9828.
(28) (a) Hirst, A. R.; Huang, B.; Castelletto, V.; Hamley, I. W.; Smith, D. K. *Chem.—Eur. J.* **2007**, *13*, 2180–2188. (b) RyongNam, S.; Lee, H. Y.; Hong, J. I. *Chem.—Eur. J.* **2008**, *14*, 6040–6043. (c) Smith, D. K. *Chem. Soc. Rev.* **2009**, *38*, 684–694.

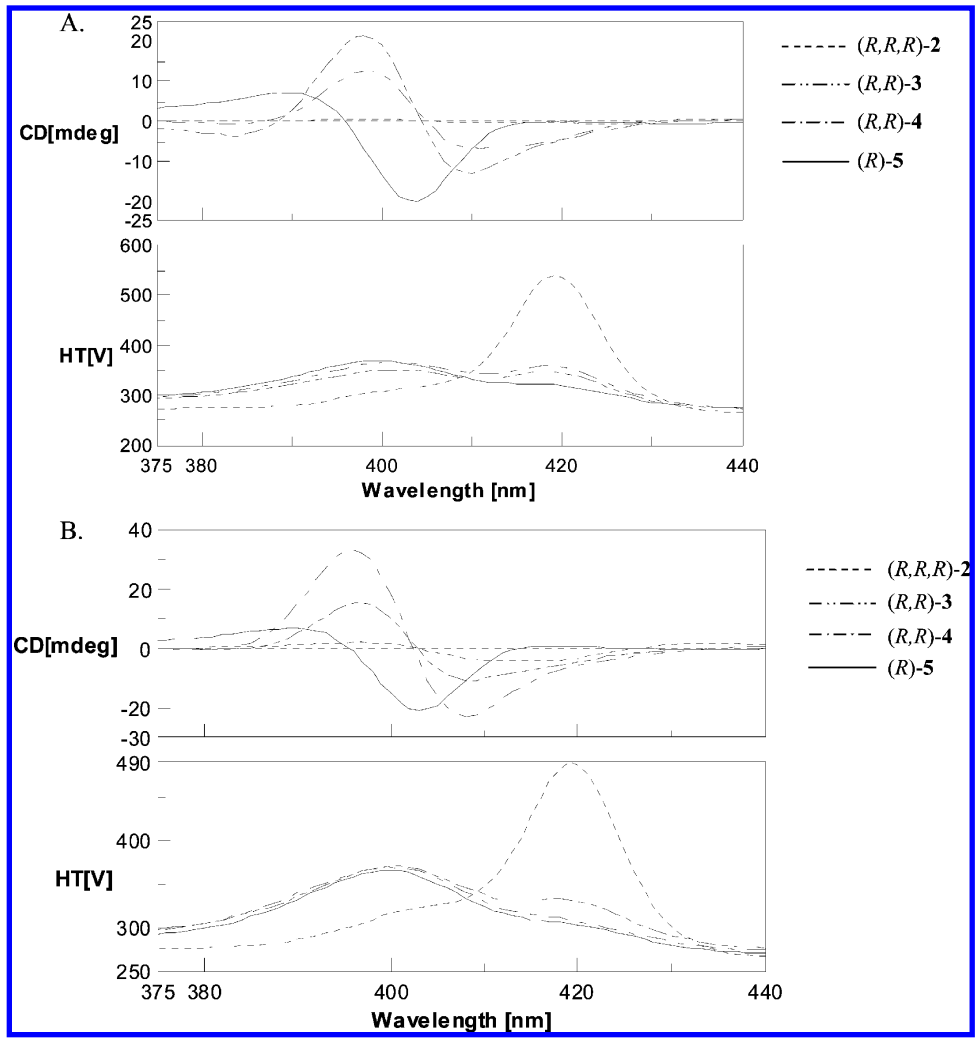

Figure 5. CD spectra (top) and corresponding absorption signal from the CD spectrometer (bottom) of compounds **2**−**5** in methylcyclohexane (1×10^{-5} M) at (A) −5 °C and (B) −10 °C.

Table 2. Positive and Negative Cotton Effects of Compounds **2**−**5** in the Spectral Region of Their B-Bands in Methylcyclohexane at −10°C

	Cotton effects, λ_{max}	
compd	negative	positive
2	413	396
3	409	397
4	408	396
5	403	389

finding indicates that at room temperature the molecules are essentially isolated in the solvent, while at lower temperatures they self-assemble into helical structures giving rise to an exciton-type CD signal.[29] Because the CD spectra exhibit a negative sign for the first Cotton effect, it means that the dipole moments (in the porphyrin chromophores) orient in an anticlockwise direction in the aggregate of the *R* enantiomers (left-handed helical structure).[30] As seen in Table 2 the optical activity of **5** is different from that of the other compounds: The Cotton effect of **5** is blue-shifted compared with the other aggregates, and this effect can be attributed to a different organization in the superstructure.

The relative intensity of the aggregated and isolated absorption signals at each temperature is different for each one of the compounds. If we consider the absorption of **2**−**5** at −5 °C, it can be observed that while **2** only starts to self-assemble into helix, **3** and **4** already have approximately half of their monomers (with a slight difference between them) in the aggregated form and **5** has almost all of its monomers in the aggregated form (Figure 5). From these observations, we can say that the free energy of interaction between the molecules diminishes as follows: **5**, **4**−**3** (with approximately the same value), and **2**. These results are supported by theoretical study (vide infra).

The sum of the maximum intensities of each Cotton effect of a split CD curve is defined as the "amplitude" (*A*), and either a positive or a negative sign is assigned to it depending on whether the highest wavelength Cotton effect is positive or negative.[31] The *A* value is proportional to ε^2 and inversely proportional to the square of the interchromophore distance (R^2)

(29) Jonkheijm, P.; van der Schoot, P.; Schenning, A. P. H. J.; Meijer, E. W. *Science* **2006**, *313*, 80–83.

(30) (a) Jung, J. H.; Ono, Y.; Shinkai, S. *Chem.—Eur. J.* **2000**, *6*, 4552–4557. (b) Jung, J. H.; Kobayashi, H.; Masuda, M.; Shimizu, T.; Shinkai, S. *J. Am. Chem. Soc.* **2001**, *123*, 8785–8789. (c) Sugiyasu, K.; Fujita, N.; Shinkai, S. *Angew. Chem., Int. Ed.* **2004**, *43*, 1229–1233. (d) S Kawano, S.; Fujita, N.; Shinkai, S. *Chem.—Eur. J.* **2005**, *11*, 4735–4742.

(31) Matile, S.; Berova, N.; Nakanishi, K.; Fleischhauer, J.; Woody, R. W. *J. Am. Chem. Soc.* **1996**, *118*, 5198–5206.

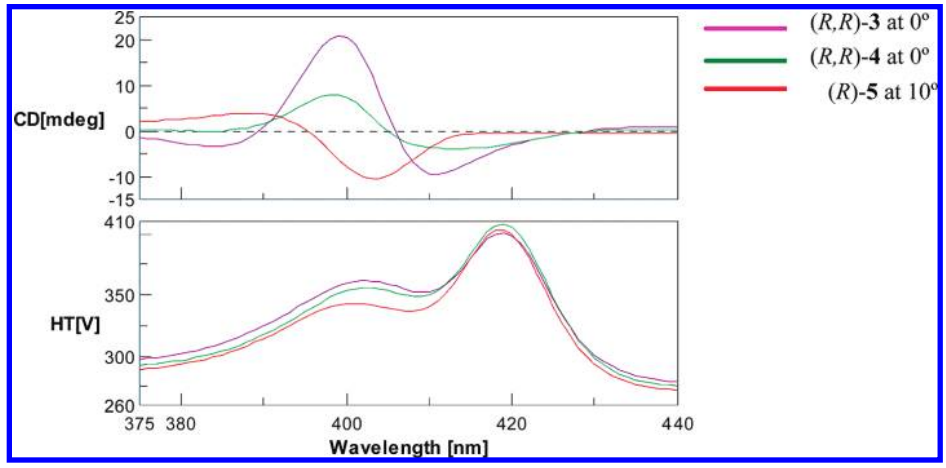

Figure 6. CD spectra (top) and corresponding absorption signal from the CD spectrometer (bottom) of compounds **3**−**5** in methylcyclohexane (1×10^{-5} M). The temperature is indicated in the figure.

Figure 7. Photograph of the gel formed by **5** in methylcyclohexane.

and has a parabolic dependence on the dihedral angle between the coupling transitions.[32] For a compound containing two or more identical chromophores, A can be estimated by the summation of each interacting pair. Thus, in a system containing three identical chromophores I/II/III, the observed amplitude can be estimated by the sum of the three interacting chromophore pairs (basis pairs): $A_{total} = A_{I,II} + A_{II,III} + A_{I,III}$.[33] At −10 °C, the value of A is −6 mdeg for **2**, −26 mdeg for **3**, −56 mdeg for **4**, and −27 mdeg for **5**. The different value of A for each compound could be related to a different length of the helical assembly where a different number of pairs interact between themselves or/and to a different structure of these helices.

Under the same conditions of concentration of the aggregated form (same absorption intensity), a symmetric exciton coupling band is observed for **3** and **4** and a dissymmetric one for **5** (Figure 6). This observation, together with the different Cotton effect values seen for **5** (see above), can be explained by a different aggregate structure of **5** when compared with the other porphyrins, where the distance and/or the angle between the chromophores is different.

Gelation Properties of the Porphyrin Derivatives. The ability of each compound with four amide groups to gelate organic solvents was studied in methylcyclohexane, which was the best solvent found for these compounds. They also gelate hexane and toluene at a similar critical gel concentration of methylcyclohexane, with the exception of compound **6** which precipitates in hexane. Methylcyclohexane is also a convenient solvent for studying the optical properties of the aggregates because it is not very volatile and is transparent in the visible and near-ultraviolet parts of the electromagnetic spectrum. The porphyrins formed clear pink gels as shown in Figure 7. The critical gel concentration of each compound is showed in Table 3.

Table 3. Critical Gel Concentrations for the *R* Enantiomers of Porphyrins **1**−**6** in Methylcyclohexane (Identical Values Are Obtained for the *S* Enantiomers)

compd	critical gel concentration (in mg/mL) of porphyrins in methylcyclohexane
(*R*,*R*,*R*,*R*)-**1**	16 (not transparent)
(*R*,*R*,*R*)-**2**	22
(*R*,*R*)-**3**	8
(*R*,*R*)-**4**	6
(*R*)-**5**	2
6	2

The enantiomers of compound **1** form a very thick and nontransparent gel-like material at 1.6 wt % in methylcyclohexane, **2** gelates the same solvent at even higher concentration than **1** (although for **2** the gel is transparent), while porphyrins **3** and **4** need three times less material than **2**. The compound

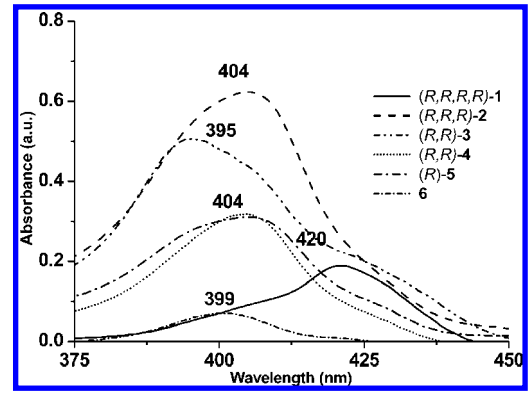

Figure 8. UV−vis absorption spectra of compounds **1**−**6** in their gel state in methylcyclohexane. The relative absorbance cannot be compared because of the different path lengths in the samples (see text).

(32) Harada, N.; Nakanishi, K. *Circular Dichroism Spectroscopy-Exciton Coupling in Organic Stereochemistry*; University Science Books: Mill Valley, CA, 1983.
(33) Nakanishi, K.; Berova, N. In *Circular Dichroism*; Nakanishi, K., Berova, N., Woody, R. W., Eds.; VCH Publishers Inc.: Weinheim, 1994; pp 361−395.

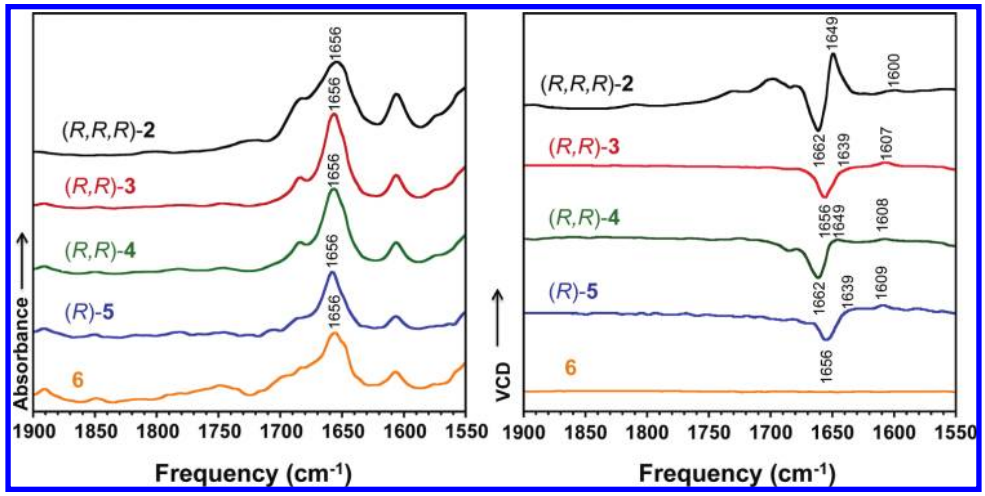

Figure 9. IR (left) and VCD (right) spectra of all studied compounds.

with only one stereogenic center (**5**) has the same critical gel concentration as the achiral compound **6**, which shares the lowest critical gel concentrations of those reported here, 0.2 wt %. It seems clear that the fewer number of stereogenic centers present in the molecule the lower is the critical gel concentration. The different critical gel concentrations of compounds **1**−**6** probably result from disturbed interactions between molecules by the methyl group attached to the stereogenic center. In fact, there is a small difference between the critical gel concentration of constitutional isomers **3** and **4** uniquely because of the position of the stereogenic center. This argument is supported by the observation of different conformations that chiral chains of a related type adopt compared with their achiral counterparts.[34] It does not take into account that, by and large, stereogenic centers can lead to increased solubility in this kind of compounds, a factor which can be important in the formation of gels[35,36] and which could also play a role in the phenomenon observed.

The gel state was not convenient for the study of the optical activity of the compounds because for some of them very high concentrations were required, leading to experimental noise as well as the possibility of birefringence effects.[37] The porphyrin concentrations in the gel were so high that the absorption spectra could not be obtained using a conventional optical cell. Thus, the gel-phase absorption spectra were measured with a gel sample sandwiched between two glass plates so that the ordinate axis is expressed with an arbitrary unit (Figure 8). The gel of enantiomerically pure compounds **2**−**6** in methylcyclohexane showed an absorption peak at about 400 nm, indicative of exciton coupling, and the formation of an H-aggregate.[38−40] Because of the less favorable conditions for compound **1** to form strong interactions between molecules, its gel in methylcyclohexane shows the Soret band and a very broad weak band shifted to the red region.

The observation of an exciton band at around 400 nm in the absorption spectra of the gels implies that the mode of aggregation is very similar to that seen in the CD experiments in solution. Indeed, it is probable that the aggregates observed at low temperature in solution are precursors in the formation of the gels.[41]

We were able to probe the structural chirality of the gels using VCD, which has emerged as a powerful chiroptical method for studying the structure of supramolecular assemblies.[42] This technique combines the advantage of vibrational spectroscopy (rich structural fingerprint region of IR absorption spectra) with conformational sensitivity. The identification of specific parts of a molecule's configuration which is influenced by chiral supramolecular aggregation is the advantage of VCD. In particular, it has been successfully applied previously to the case of the gelation process of a porphyrin.[41]

The IR absorption and VCD spectra of the gels under study here are shown in Figure 9. The IR spectra are dominated by a strong signal at 1656 cm^{-1} assigned to the C═O stretching mode of the amide groups (amide I) and is equally observed in the chiral and nonchiral porphyrins.

The VCD spectra show that all the chiral compounds with between one and three stereocenters show a signal at the position of the amide I band. The achiral molecule is CD silent, and the gel containing the compound with four stereocenters is too concentrated to be studied. The signal in the region of the amide I band is a result of chiral induction caused by aggregation, since when a nonaggregated form is studied by VCD a negative band centered on 1721 cm^{-1} is observed (which corresponds to a band in the IR spectrum).

(34) De Feyter, S.; Gesquiere, A.; Wurst, K.; Amabilino, D. B.; Veciana, J.; De Schryver, F. C. *Angew. Chem., Int. Ed.* **2001**, *40*, 3217–3220.
(35) Hirst, A. R.; Coates, I. A.; Boucheteau, T. R.; Miravet, J. F.; Escuder, B.; Castelletto, V.; Hamley, I. W.; Smith, D. K. *J. Am. Chem. Soc.* **2008**, *130*, 9113–9121.
(36) Pham, Q. N.; Brosse, N.; Frochot, C.; Dumas, D.; Hocqueta, A.; Jamart-Gregoire, B. *New J. Chem.* **2008**, *32*, 1131–1139.
(37) (a) Shindo, Y.; Ohmi, Y. *J. Am. Chem. Soc.* **1985**, *107*, 91–97. (b) Livolant, F.; Maestre, M. F. *Biochemistry* **1988**, *27*, 3056–3068. (c) Kuroda, R.; Harada, T.; Shindo, Y. *Rev. Sci. Instrum.* **2001**, *72*, 3802–3810. (d) Yao, H.; Isohashi, T.; Kimura, K. *Chem. Phys. Lett.* **2004**, *396*, 316–322.
(38) Shirakawa, M.; Kawano, S.; Fujita, N.; Sada, K.; Shinkai, S. *J. Org. Chem.* **2003**, *68*, 5037–5044.
(39) Choi, M. S. *Tetrahedron Lett.* **2008**, *49*, 7050–7053.
(40) De Luca, G.; Romeo, A.; Villari, V.; Micali, N.; Filtran, I.; Foresti, E.; Lesci, I. G.; Roveri, N.; Zuccheri, T.; Scolaro, M. S. *J. Am. Chem. Soc.* **2009**, *131*, 6920–6921.
(41) Král, V.; Pataridis, S.; Setnička, V.; Záraba, K.; Urbanová, M.; Volka, K. *Tetrahedron* **2005**, *61*, 5499–5506.
(42) Smulders, M. M. J.; Buffeteau, T.; Cavagnat, D.; Wolffs, M.; Schenning, A. P. H. J.; Meijer, E. W. *Chirality* **2008**, *20*, 1016–1022.

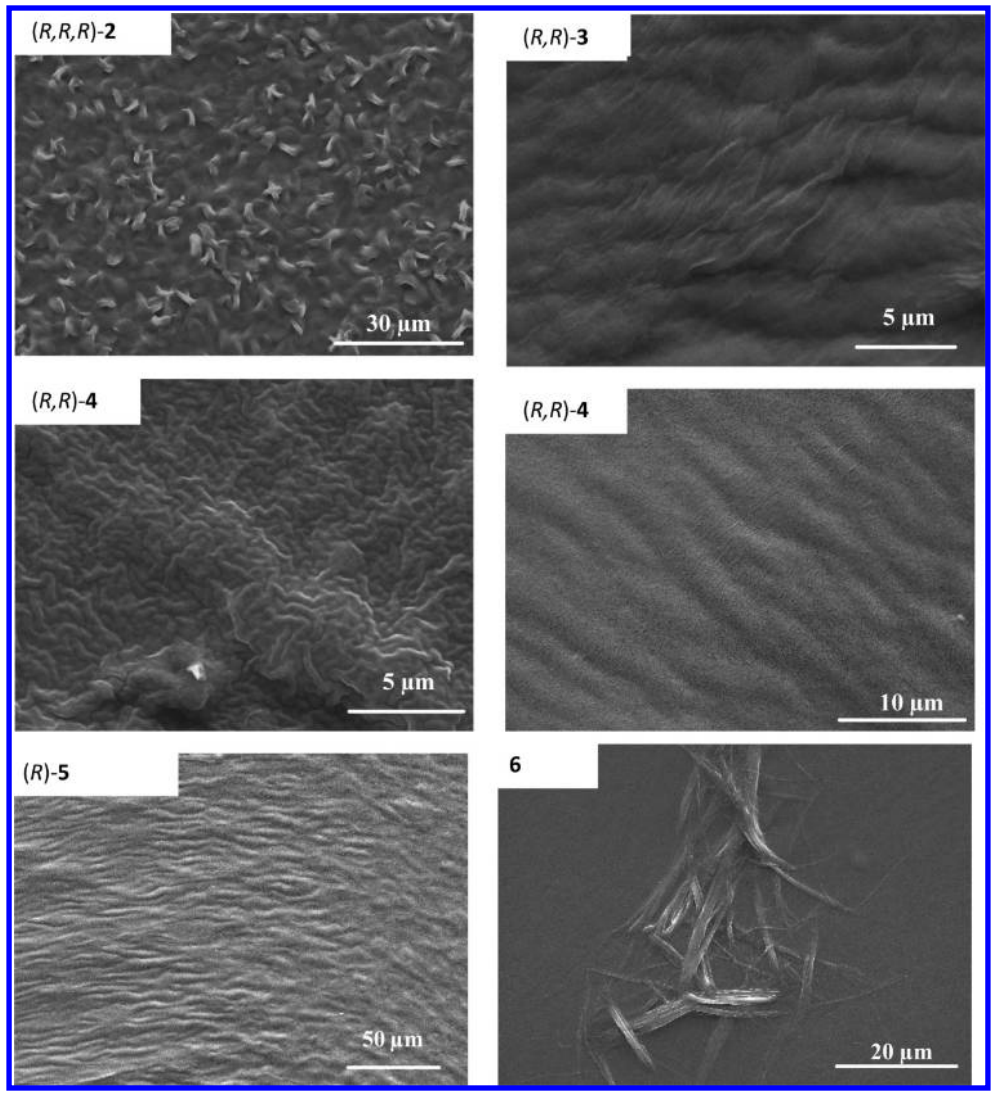

Figure 10. SEM images of xerogels of (*R*,*R*,*R*)-**2**, (*R*,*R*)-**3**, (*R*,*R*)-**4**, (*R*)-**5**, and **6** on glass.

Linear dichroism is a potential issue,[43] but this has been ruled out in our case by repeating the spectra on different gel samples of the same compound and by recording the spectra at different angles. The quality of the data is judged to be good because the achiral compound shows no VCD signal and the enantiomers show mirror image spectra.

For the chiral compounds, we observe that the VCD spectra display more variations in the series than the IR absorptions. On the one hand, only the gel of (*R*,*R*,*R*)-**2** shows a well-defined bisignate band at (−)1662/(+)1649 cm^{-1} that indicates a twisted secondary structure of the aggregate. On the other hand, the other samples display a strong negative signal. The frequencies of the bands for compounds (*R*,*R*,*R*)-**2** and (*R*,*R*)-**4** show the negative component at 1662 cm^{-1}, while (*R*)-**5** and (*R*,*R*)-**3** show this signal at 1656 cm^{-1}. There is a connection between the frequency position and the intermolecular interactions in the aggregated gels which produces these two-to-two similarities and differences. Moreover, only in (*R*,*R*)-**4**, which is paired in frequency with (*R*,*R*,*R*)-**2**, is a positive signal related with the strong negative one observed corroborating that aggregation in both samples might follow a similar pattern.

A weak positive chiral signal in the four samples in the 1600−1610 cm^{-1} range is observed showing a noticeable frequency downshift from (*R*)-**5** (1609 cm^{-1}), (*R*,*R*)-**4** (1608 cm^{-1}), and (*R*,*R*)-**3** (1607 cm^{-1}) to (*R*,*R*,*R*)-**2** (1600 cm^{-1}). Considering that this vibrational mode corresponds to the C═C stretching bands of the tetrapyrrole core, the stacking and helicoidal-like aggregation might be the reasons for its VCD signal. In conclusion, the different ways of inducing chirality in these porphyrin systems are nicely detected in the VCD spectra of the gels.

Morphology of Xerogels. The morphology of the dried gels (xerogels) of all compounds was investigated by optical microscopy and SEM on a glass slide and by SFM on HOPG. Compound **1** does not form a transparent gel, and an irregular porous morphology formed when it is deposited onto glass, dried, and observed through an optical microscope (see the Supporting Information). The gel from **2** forms a porous structure of disordered fibers. The gels from **3**−**6** present essentially the same morphology, which is constituted of fibers with relatively long-range uniform orientation. A bigger difference in the morphology of the xerogels can be observed from SEM images (Figure 10). The achiral porphyrin **6** forms well separated and oriented fibers, while **3**−**5** give bundles of oriented fibers and **2** gives disordered bundles of fibers as in the optical

(43) Brizard, A.; Berthier, D.; Aime, C.; Buffeteau, T.; Cavagnat, D.; Ducasse, L.; Huc, I.; Oda, R. *Chirality* **2009**, *21*, S153–S162.

microscope, which seem to form a porous material. In some cases, in areas of higher xerogel concentration, **5** gives more disordered fibers.

In order to obtain a thin film easy to study by SFM (deposition of lumps of the gels gives an extremely rough surface), the porphyrin layer was formed after casting a drop of the hot solution of the corresponding compound in methylcyclohexane onto graphite and leaving it to cool to room temperature. The dry gels on graphite appear as randomly distributed overlapped fibers whose width goes from 20 to 200 nm, and the roughness of the SFM images is in the range 3.5−6.0 nm. (Figure 11). It is not possible to ascertain the height of the fibers from these images because of the density of the structures which touch and overlap. A qualitative difference can be observed in the images of xerogels **2**−**6**. Compounds **5** and **6** appear as bundles of long fibers, whereas **2**−**4** form more random distributed shorter fibers. No relevant images could be recorded for **1**, probably because of the tendency of the compound to form large irregular aggregates and not self-assemble into superstructures with long-range order.

To put the morphology of the gels of these porphyrins into context, in materials formed by other organogelators much better defined fibers are usually observed, and these objects are not as bundled as the ones seen here. The compound with the most classical morphological features is **6**, but even this compound shows mainly bundled fibers. Two features distinguish the organogelators discussed here from more habitual systems. First, their molecular weight is relatively large. Most compounds described in the literature have molecular weights below 1000 Da. Second, and perhaps more importantly, the symmetry of the porphyrins is different from most organogelators: the porphyrins are (pseudo) C_4-symmetric, a shape which often promotes discotic assemblies, while other gels are comprised of calamitic (rod-shaped) molecules. The latter can form smectic (layer-like) assemblies, which might encourage film formation. On the other hand, discotic-type molecules can, in principle, interact uniformly in all directions perpendicular to the disk-stacking direction. This effect might also explain the lack of any observation of helices in the images obtained of these chiral fiber containing materials. At the very least, the domain sizes are much smaller than most gels reported in the literature, and the small coherence length will cause the systems to require a high concentration of gelator before immobilization of the solvent takes place.

Molecular Modeling Study of Porphyrin Aggregation. The self-assembly into helical stacks of the fully chiral and fully achiral porphyrin (derivatives **1** and **6**, respectively) were modeled using periodic boundary conditions in order to avoid edge effects.[44] Because of the C_2 symmetry of the molecules (caused by the localization of the pyrrolic protons), it is only necessary to rotate them by 180° to retrieve a situation identical to the initial one. For the achiral porphyrin (**6**), it is possible to build two different helices: a clockwise (CW) helix and a counterclockwise (CCW) helix (Figure 12). For each of these two helices, the pitch angle is about 2.4° resulting in 74 porphyrin molecules in the periodic box. The intermolecular distances are about 4.6 Å, resulting in a box with a length of 34.5 nm.

As illustrated in Figure 12 (bottom), three main interactions drive the assembly between the porphyrin molecules: the $\pi-\pi$ interactions between the porphyrin cores, the hydrogen bonds between the amide groups and the van der Waals interactions between the alkyl chains. The combination of these three interactions provides a strong cohesion to the structures, and the stabilization in these stacks is found to be 56.9 kcal/mol per porphyrin molecule for both CW and CCW assemblies.

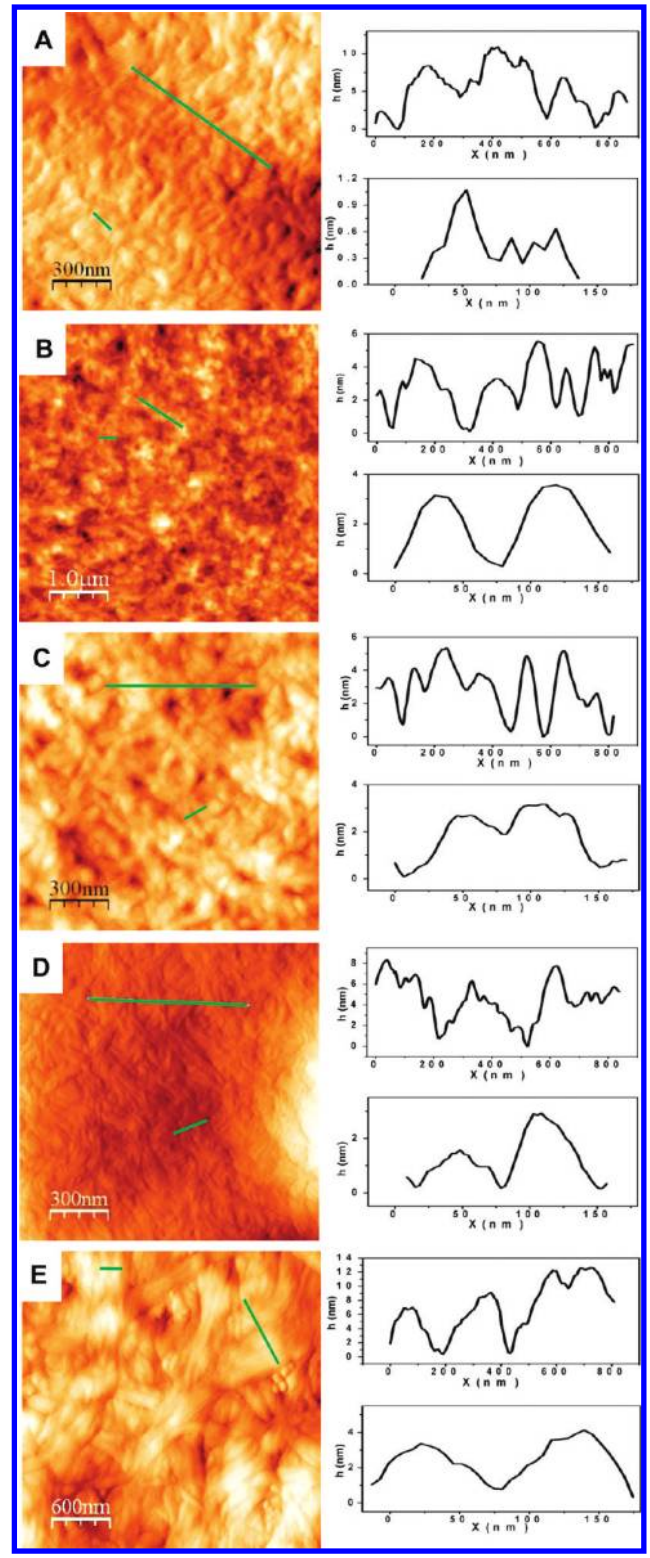

Figure 11. SFM images of xerogels from methylcyclohexane of (A) (*R*,*R*,*R*)-**2**; (B) (*R*,*R*)-**3**; (C) (*R*,*R*)-**4**; (D) (*R*)-**5**; (E) **6**.

Starting from the two helices (CW and CCW) obtained with the achiral porphyrin **6**, the two corresponding stacks of **1** were built and the structures were optimized. The methyl group on the stereogenic center has a major influence on the packing. Upon optimization, two different situations appear: a well organized structure is maintained in the counterclockwise helix

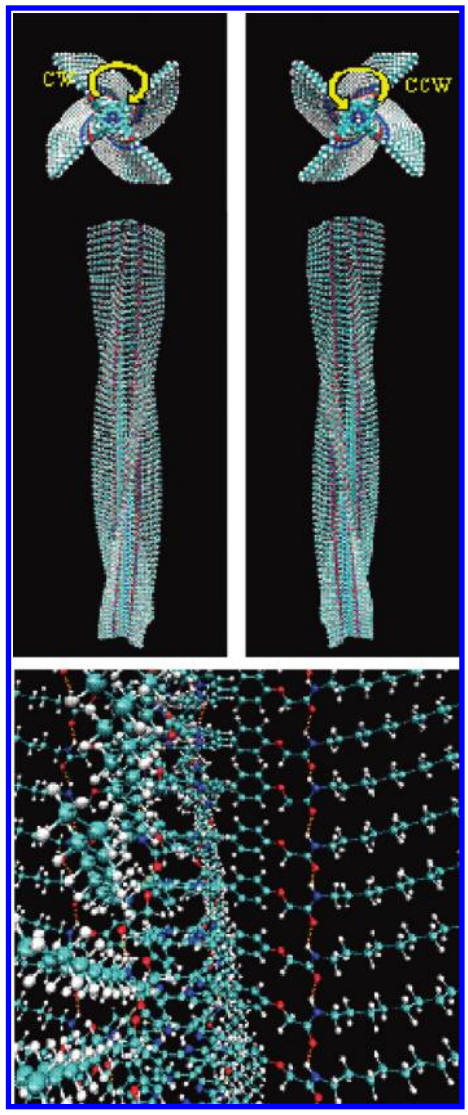

Figure 12. Illustrations of the model of the helix formed by **6**. Top: Top and side views of the CW and CCW helices. Bottom: A view of the $\pi-\pi$ stacking between the porphyrin cores and the hydrogen bonds between the amide groups.

(Figure 13A), whereas a more disordered structure is observed for the initially clockwise helix (Figure 13B,C).

This result indicates that for compound **1** the CCW arrangement is much more stable than the CW arrangement; indeed, the stabilization energy is 59.5 kcal/mol per molecule in the CCW arrangement but only 49.3 kcal/mol per molecule in the CW arrangement. This preference is a direct result of the steric hindrance caused by the methyl group on the chiral center, which disturbs the formation of hydrogen bonds between adjacent porphyrin molecules in the CW helix. We also optimized and computed the stabilization energies for both CW and CCW helices for compounds **2**−**5** (to build these helices, we use a random distribution of all the possible situations: chiral centers on top of each other or alternated). The results are summarized in Figure 14, which presents the stabilization energy per molecule for the CW and CCW helices for compounds **1**−**6**.

In the CW helix, the insertion of methyl group(s) on the chiral center(s) creates an increasing steric hindrance and breaks hydrogen bonds; this is the reason why the stabilization energy becomes smaller when one increases the number of chiral centers (from 56.9 to 49.3 kcal/mol per molecule). For the CCW, the introduction of the methyl group induces a slight change in the position of the amide group, toward a more stable conformation. This movement explains why the stabilization energy increases slightly with increasing number of chiral centers (from 56.9 to 59.5 kcal/mol.molecule). This observation is in perfect agreement with the CD measurements which show the formation of a left-handed (CCW) helix for the *R* enantiomers of compounds **2**−**5** dissolved in methylcyclohexane. Moreover, the calculations indicate that the pitch of the helix does not change with the introduction of a chiral center. The observed lower aggregation propensity of the molecules with more stereocenters is therefore ascribed to the greater solubility of the compounds in methylcyclohexane, in line with other work in organogels.

Conclusions

The synthetic strategy developed for the preparation of porphyrins containing between one and four stereogenic centers provides compounds which are extremely useful for the study of chiral induction phenomena in a range of systems. In this paper, we have reported the study of low dimensional systems, in the form of fibrous aggregates and monolayers, and have found that the number of stereogenic centers has a profound effect on the optical activity, self-assembly and chiral structure of the porphyrin molecules described here.

In the self-assembled fibers, the four hydrogen bonds induce the formation of a hydrogen bonded aggregate, as witnessed by the blue-shifted exciton band, and CD measurements indicate

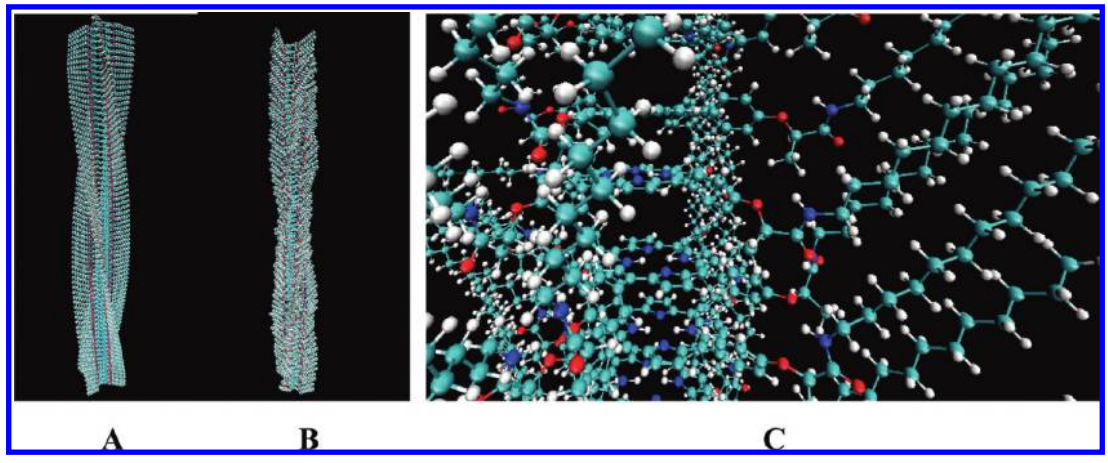

Figure 13. Model of **1** self-assembled into the helix: side view of the CCW helix (A), side view of the CW helix (B), close-up on the CW helix (C) showing that the methyl group on the chiral center disturbs the formation of hydrogen bonds.

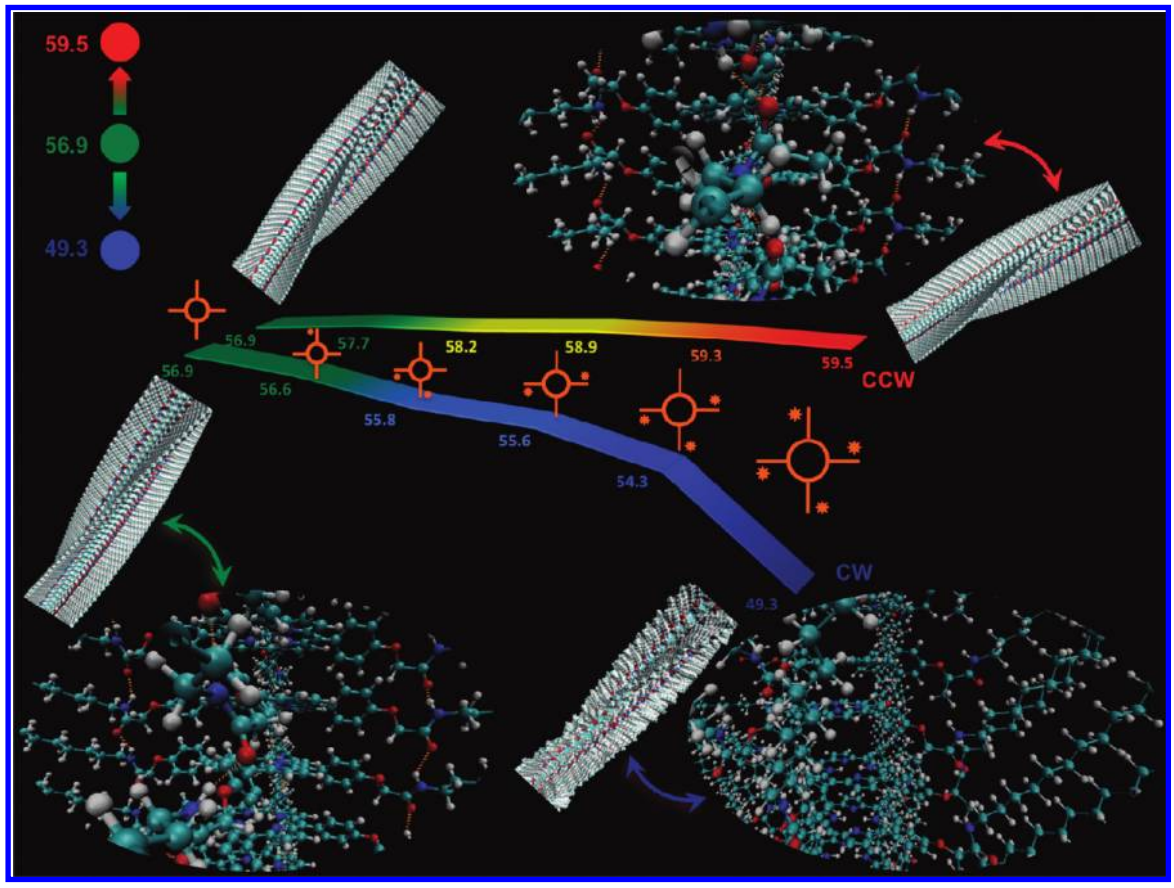

Figure 14. Stabilization energy per molecule (kcal/mol) for the CW and CCW helices for the *R* enantiomers of compounds **1**−**5** and achiral compound **6**.

that these compounds self-assemble in solution into helical structures. The nature and stability of the aggregates depend critically on the number of stereocenters.

At sufficiently high concentrations the chiral porphyrin derivatives are able to gelate methylcyclohexane, and this property depends on the number and position of chiral groups at the periphery of the aromatic core, reflecting the different aggregation forces of the molecules in solution. The single methyl group allows the compound to form a gel at a relatively low concentration (1.18×10^{-3} M). We found the conditions needed for forming a chiral gel at the same concentration as the corresponding achiral derivative gelates were the same, while an increased number of stereogenic centers required more material, in all likelihood because of their greater solubility.[35] Another possible contribution to the reduced ability of the compound with four stereogenic centers to form aggregates could be steric interactions resulting in a mismatch penalty,[45] although our calculations on the H-aggregates formed here do not point to such an effect.

The SFM and SEM analyses of the gels showed the aggregates to have very similar morphology. We believe that this absence of morphological chirality is a result of the long pitch and symmetry of these discotic-type systems, an unusual one in organogel systems which are usually based on calamitic molecules.

In the two-dimensional systems, the degree of structural chirality with respect to reference surface axes increases almost linearly with the number of stereogenic centers, and only one handedness is formed in the monolayers, whereas the achiral compound forms a mixture of mirror-image domains at the surface.

The presence of only one stereogenic center is enough to induce single-handed chirality in the self-assembled structures in both the one and two-dimensional supramolecular structures, in which the relative orientation of the molecules is completely different, pointing therefore to a common effect.

Acknowledgment. This work was supported by the European Union Marie Curie Research Training Network CHEXTAN (MRTN-CT-2004-512161) and NoE MAGMANet (515767-2) and NMP4-CT-2006-032109 (STREP "SURMOF"), the Dirección General de Investigación, Ciencia y Tecnología (Spain, Project Nos. MAT2007-62732, and CTQ2009-10098), the Junta de Andalucia (Grant No. FQM-0159, Project No. P09-4708), and the DGR, Catalonia (Project No. 2009 SGR 158). The collaboration between Leuven and Mons is supported by the Science Policy Office of the Belgian Federal Government (PAI 6/27). Research in Mons is also supported by FRS-FNRS. We warmly thank Amable Bernabé at the ICMAB for recording IR and LDI-TOF spectra. We also thank the reviewers for constructive criticism which helped improve the quality of the article.

Supporting Information Available: Full experimental section including a description of the synthesis and characterization of all new materials and all the techniques employed in the research reported here and figures showing variable-temperature CD and UV−vis absorption spectra, optical micrographs of the gels, and NMR spectra of the isomers **11** and **12**. This material is available free of charge via the Internet at http://pubs.acs.org.

JA101533J

(44) Iavicoli, P.; Linares, M.; Pérez del Pino, A.; Lazzaroni, R.; Amabilino, D. B. *Superlattices Microstruct.* **2008**, *44*, 556–562.
(45) Smulders, M. M. J.; Filot, I. A. W.; Leenders, J. M. A.; van der Schoot, P.; Palmans, A. R. A.; Schenning, A. P. H. J.; Meijer, E. W. *J. Am. Chem. Soc.* **2010**, *132*, 611–619.